



Contents lists available at ScienceDirect

Corrosion Science

journal homepage: [www.elsevier.com/locate/corsci](http://www.elsevier.com/locate/corsci)



## Hot corrosion behavior of $\text{LaTi}_2\text{Al}_9\text{O}_{19}$ ceramic exposed to vanadium oxide at temperatures of 700–950 °C in air

Xin Zhou<sup>a,b,c</sup>, Zhenhua Xu<sup>c</sup>, Limin He<sup>c</sup>, Jiaying Xu<sup>a,b</sup>, Binglin Zou<sup>a,\*</sup>, Xueqiang Cao<sup>a,\*</sup>

<sup>a</sup> State Key Laboratory of Rare Earth Resource Utilization, Changchun Institute of Applied Chemistry, Chinese Academy of Sciences, Changchun 130022, China

<sup>b</sup> University of Chinese Academy of Sciences, Beijing 100049, China

<sup>c</sup> Beijing Institute of Aeronautical Materials, Department 5, Beijing 100095, China

### ARTICLE INFO

#### Article history:

Received 12 October 2015

Received in revised form

26 December 2015

Accepted 29 December 2015

Available online xxx

#### Keywords:

A. Ceramic

A. Molten salts

C. Hot corrosion

### ABSTRACT

Hot corrosion behavior of  $\text{LaTi}_2\text{Al}_9\text{O}_{19}$  ceramic exposed to  $\text{V}_2\text{O}_5$  at 700–950 °C were investigated in order to better understand the corrosion resistance of  $\text{LaTi}_2\text{Al}_9\text{O}_{19}$  as a promising thermal barrier coating material. Results indicate that the degradation processes were significantly temperature dependent. At 700 °C,  $\text{AlVO}_4$ ,  $\text{LaVO}_4$  and  $\text{TiO}_2$  were the main corrosion products, while  $\text{AlVO}_4$  partially decomposed at 800 °C to form  $\theta\text{-Al}_2\text{O}_3$  and  $\alpha\text{-Al}_2\text{O}_3$ . After exposure to 950 °C,  $\text{V}_2\text{O}_5$  reacted with  $\text{LaTi}_2\text{Al}_9\text{O}_{19}$  to form  $\text{LaVO}_4$ ,  $\alpha\text{-Al}_2\text{O}_3$  and  $\text{TiO}_2$  as final corrosion products. The hot corrosion mechanisms were further discussed based on the phase diagrams of  $\text{V}_2\text{O}_5\text{--Al}_2\text{O}_3$ ,  $\text{V}_2\text{O}_5\text{--La}_2\text{O}_3$  and  $\text{V}_2\text{O}_5\text{--TiO}_2$  systems.

© 2015 Elsevier Ltd. All rights reserved.

### 1. Introduction

Thermal barrier coatings (TBC) are widely used in aircraft engines and land-based gas turbines to provide thermal, corrosion and erosion protections for the critical metallic components (blades, vanes and combustor chambers) [1,2]. State-of-the-art TBC consists of a NiPtAl diffusion or NiCrAlY overlay bond coat (BC) as oxidation resistant layer and a ceramic topcoat for thermal insulation [2,3]. Up to now, most of the investigations and applications of the ceramic topcoat for TBC have focused on 6–8 wt.% yttria stabilized zirconia (YSZ) due to its low thermal conductivity and comparative thermal expansion coefficient with the superalloy substrate etc [4–6]. However, the maximum operation temperature of YSZ is limited to 1200 °C for long-term application. At higher temperatures, YSZ coating suffers serious sintering and martensitic phase transformation accompanied by a 4–6% volume expansion, which could lead to early spallation of TBC [1,2,7]. An additional concern regarding the degradation of the TBC apart from the aforementioned phase transformation and sintering issues is the presence of molten salt contaminants such as Na, S and V originating from fuel impurities [2,8,9]. During operation, YSZ coatings are prone to hot corrosion caused by molten sulfate and vanadate

salts which condense on the TBC at the temperature of 600–1000 °C [10,11]. The yttria stabilizer will leach out of zirconia by the reactions with  $\text{V}_2\text{O}_5$  or  $\text{NaVO}_3$  to form  $\text{YVO}_4$ , resulting in the structural destabilization of  $\text{ZrO}_2$ , which would impose an accelerated degradation and spallation of the YSZ coating during high temperature service [2,11]. As a result, extensive efforts have been devoted to the development of ceramic materials with improved phase stability and corrosion resistance for TBC applications. For instance, metal oxides such as  $\text{CeO}_2$ ,  $\text{Ta}_2\text{O}_5$  and  $\text{Re}_2\text{O}_3$  (Re = La, Nd, Sm, Gd, Yb and Sc) were incorporated into the  $\text{ZrO}_2$ -base solid solution as the new stabilizer or co-stabilizer in terms of higher phase stability and hot corrosion resistance [2,11–15]. On the other hand, new TBC candidate materials such as pyrochlores ( $\text{Re}_2\text{Zr}_2\text{O}_7$ , Re = La, Nd, Sm and Gd) [16,17], perovskites ( $\text{SrZrO}_3$ ,  $\text{BaZrO}_3$ ,  $\text{BaLa}_2\text{Ti}_3\text{O}_{10}$ ) [16,18] and fluorite-type  $\text{Re}_2\text{Ce}_2\text{O}_7$  (Re = La and Nd) [19] have also been evaluated for potential applications.

$\text{LaMgAl}_{11}\text{O}_{19}$  (LaMA) with magnetoplumbite-type structure as a new TBC candidate material has attracted enormous interest due to its outstanding sintering resistance, high fracture toughness, as well as the high temperature phase stability [1,2,20]. Previous studies indicated that the plasma sprayed LaMA coating exhibited a good thermal cycling lifetime and superior hot corrosion resistance to the traditional YSZ coating [21,22], however, the relative high thermal conductivity of LaMA was the major obstacle for these coatings to be used as ideal TBC for future ultra-efficient and low-emission engine systems [23].

\* Corresponding authors. Fax: +86 10 62496456.

E-mail addresses: [zoubinglin@ciac.ac.cn](mailto:zoubinglin@ciac.ac.cn) (B. Zou), [xcao@ciac.ac.cn](mailto:xcao@ciac.ac.cn) (X. Cao).

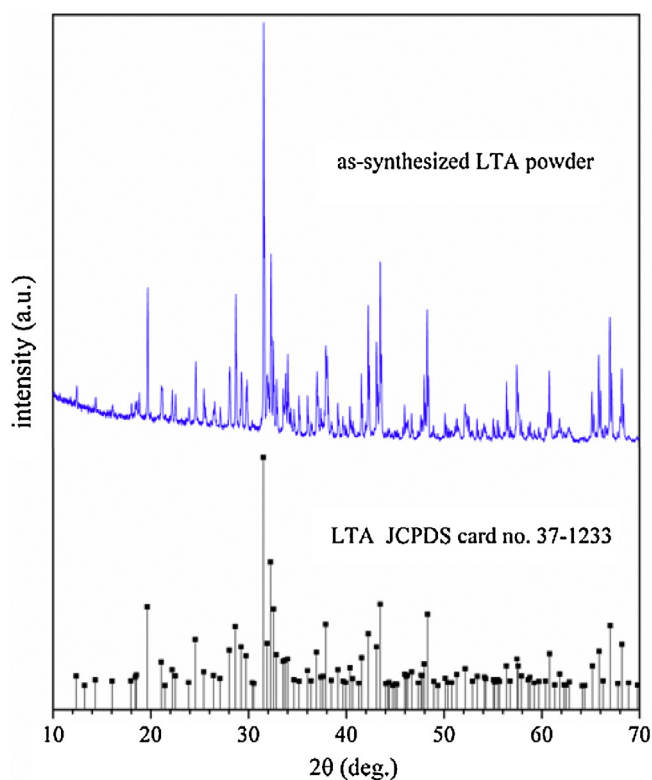


Fig. 1. XRD pattern of as-synthesized LTA powder.

Recently, Lanthanum titanium aluminum oxide ( $\text{LaTi}_2\text{Al}_9\text{O}_{19}$ , LTA) has been proposed as a new TBC candidate [24–26]. LTA is featured with a huge unit cell which is four times as large as that of the magnetoplumbite phase [24]. The complex atoms arrangement and lower symmetry of the LTA crystallographic structure could allow achieving the capability of a lower thermal conductivity [24]. As reported by Xie et al. [24], LTA showed phase stability up to  $1600^\circ\text{C}$  and the thermal conductivities for LTA coating were in a range of  $1.0\text{--}1.3\text{ W m}^{-1}\text{ K}^{-1}$  ( $300\text{--}1500^\circ\text{C}$ ), which was much lower than those of LaMA ( $2\text{ W m}^{-1}\text{ K}^{-1}$ ,  $1200^\circ\text{C}$ ). Meanwhile, LTA also showed a moderate thermal expansion coefficient, close to  $\sim 11.2 \times 10^{-6}\text{ K}^{-1}$  at  $1400^\circ\text{C}$ . Thermal cycling experiment results [25] indicated that the plasma-sprayed LTA/YSZ double ceramic layer TBC exhibited lifetime of more than 4000 cycles when the sample surface was heated by gas flame to  $1300^\circ\text{C}$ . LTA coating also showed a good chemical stability with the molten salt of  $\text{Na}_2\text{SO}_4$  and  $\text{NaCl}$  in hot corrosion test [27]. However, no date on the phase evolution and microstructure of LTA ceramic upon high temperature exposure to molten vanadium oxide is available in open literatures.

In the current work, the hot corrosion behavior of LTA ceramic exposed to molten  $\text{V}_2\text{O}_5$  at  $700\text{--}950^\circ\text{C}$  was investigated in order to understand the corrosion resistance of LTA as a promising material for TBC applications. The related corrosion mechanisms are also discussed.

## 2. Experimental procedure

LTA powders were synthesized by solid state reaction using  $\text{La}_2\text{O}_3$  (99.99%),  $\text{TiO}_2$  (99.7%) and  $\gamma\text{-Al}_2\text{O}_3$  (99.99%) as the starting materials at  $1550^\circ\text{C}$  for 12 h. As shown in Fig. 1, the XRD pattern of as-synthesized LTA powder well matches the corresponding LTA JCPDS card no. 37-1233 [28], indicating a good purity. The as-synthesized LTA powders were uniaxially compacted at 20 MPa, followed by pressureless-sintering at  $1650^\circ\text{C}$  for 24 h. The sintered

specimens were shaped using mechanical grinding and then the bulk densities were determined by mass and dimensions measurements. Theoretical density available in the literature [28] was used to calculate the relative densities. The measured bulk densities were  $\sim 3.4\text{ g/cm}^3$  and the relative densities of the specimens were  $\sim 80\%$  compared with theoretical density  $4.300\text{ g/cm}^3$  of the LTA. The porous specimens have a similar porosity to the corresponding coatings prepared either by atmospheric plasma spraying (APS) or electron-beam physical deposition (EB-PVD) methods, which are more representative of TBC than dense samples.

Hot corrosion tests were carried out in a muffle furnace. Before hot corrosion experiment, the specimens were ground by 600 grit sandpaper, followed by ultrasonic cleaning in ethanol, and oven drying at  $100^\circ\text{C}$ . After that,  $\text{V}_2\text{O}_5$  powders with average particle size of about  $8.7\text{ }\mu\text{m}$  were uniformly spread over the specimen surface with dimensions of  $12\text{ mm} \times 12\text{ mm}$  by using a very fine glass rod. The weight of the specimen was determined by analytical balance before and after  $\text{V}_2\text{O}_5$  powders were spread. Finally, the specimens were coated with  $0.0288 \pm 0.005\text{ g}$  of  $\text{V}_2\text{O}_5$  powders, and so the concentration of  $\text{V}_2\text{O}_5$  powders on the specimen surface was calculated to be about  $20\text{ mg/cm}^2$ . Then the specimens were subjected to isothermal heat treatment at temperatures of  $700^\circ\text{C}$ ,  $800^\circ\text{C}$  and  $950^\circ\text{C}$  for 2 h and 10 h, respectively. After isothermal corrosion, specimens were cooled down to the room temperature in the furnace.

The phase analyses of LTA ceramic before and after hot corrosion test were performed by using an X-ray diffractometer (XRD, Bruker D8 Advance, Germany) with  $\text{Cu K}\alpha$  radiation. Surface and cross-section of the corroded specimens were coated by a thin Au layer to make them electro-conductive prior to examinations by using scanning electron microscopy (SEM, FEI-Quanta 600 and XL-30 FEG) equipped with energy dispersive spectroscopy.

## 3. Results

### 3.1. X-ray diffraction (XRD) analysis

XRD analysis was performed on the surface of the LTA ceramic bulk samples before and after hot corrosion tests. As can be seen in Fig. 2, the XRD pattern of as-sintered LTA bulk has no other peaks as compared to that of the LTA powder. After the LTA bulk corroded at  $700^\circ\text{C}$  for 2 h, the strong peaks ascribed to the original  $\text{V}_2\text{O}_5$  (JCPDS File no. 65-0131 [29]) and LTA phases can be clearly observed, as shown in pattern A in Fig. 2a. Besides, chemical reactions between the LTA ceramic and  $\text{V}_2\text{O}_5$  at  $700^\circ\text{C}$  resulted in the formation of a new  $\text{AlVO}_4$  phase (JCPDS File no. 39-0276 [30]). However, this  $\text{AlVO}_4$  phase has very low relative intensities, indicating that the LTA ceramic bulk only suffered a slight degradation by  $\text{V}_2\text{O}_5$  at  $700^\circ\text{C}$  during 2 h corrosion duration. When the corrosion duration was extended to 10 h, the original  $\text{V}_2\text{O}_5$  and unreacted LTA are still the main phases appearing in the corroded sample surface, but the intensity of  $\text{AlVO}_4$  phase increases remarkably with the increase of the corrosion duration (pattern A in Fig. 2b). Moreover, newly evolved peaks related to  $\text{LaVO}_4$  (JCPDS File no. 50-0367 [31]) and  $\text{TiO}_2$  (JCPDS File no. 65-1119 [32]) can also be identified. Those mean that the LTA bulk suffered more serious corrosion degradation at  $700^\circ\text{C}$  for 10 h compared with the case for 2 h.

Pattern B in Fig. 2a shows the XRD pattern of the LTA ceramic exposed to  $\text{V}_2\text{O}_5$  at  $800^\circ\text{C}$  for 2 h in air. Two new phases of  $\alpha\text{-Al}_2\text{O}_3$  (JCPDS File no. 46-1212 [33]) and  $\theta\text{-Al}_2\text{O}_3$  (JCPDS File no. 23-1009 [34]) are found in addition to  $\text{AlVO}_4$ ,  $\text{LaVO}_4$  and  $\text{TiO}_2$  according to the XRD analysis. Peaks ascribed to the original  $\text{V}_2\text{O}_5$  and unreacted LTA are still present but their relative intensities obviously decrease with the increase of the corrosion temperature from  $700$  to  $800^\circ\text{C}$ . When the corrosion duration increased to 10 h at  $800^\circ\text{C}$ , the main

Download English Version:

<https://daneshyari.com/en/article/7894924>

Download Persian Version:

<https://daneshyari.com/article/7894924>

[Daneshyari.com](https://daneshyari.com)